Broadband mode division multiplexer using all-fiber mode selective couplers

Kyung Jun Park,[1,*] Kwang Yong Song,[2] Young Kie Kim,[3] Jae Hyeon Lee,[3] and Byoung Yoon Kim[1]

[1]*Department of Physics, KAIST, 291, Daehak-ro, Yuseong-gu, Daejeon, 34141, South Korea*
[2]*Department of Physics, Chung-Ang University, 84, Heukseok-ro, Dongjak-gu, Seoul, 06974, South Korea*
[3]*KS Photonics, 28, Daehak-ro, Yuseong-gu, Daejeon, 34186, South Korea*
[*]*brainpkj@gmail.com*

Abstract: We report an all-fiber mode division multiplexer formed with cascaded mode selective couplers with significantly broadened bandwidth potentially spanning S, C and L band. This was achieved by matching the effective refractive indices over a wide wavelength range for the few mode fiber and the single mode fiber used in the coupler. The multiplexer provides high coupling efficiency (>55% for the worst case) for the 4 spatial modes over the entire wavelength range of 1515-1590 nm. The all-fiber construction provides mechanical stability. Experimental results for the coupling efficiency and the mode extinction ratio for each spatial mode are presented along with the far field radiation patterns.

©2016 Optical Society of America

OCIS codes: (060.2330) Fiber optics communications; (060.2340) Fiber optics components; (060.4230) Multiplexing; (060.4510) Optical communications.

References and links

1. R. W. Tkach, "Scaling optical communications for the next decade and beyond," Bell Labs Tech. J. **14**(4), 3–9 (2010).
2. D. J. Richardson, J. M. Fini, and L. E. Nelson, "Space-division multiplexing in optical fibres," Nat. Photonics **7**(5), 354–362 (2013).
3. R. Ryf, R. Essiambre, A. Gnauck, S. Randel, M. A. Mestre, C. Schmidt, P. Winzer, R. Delbue, P. Pupalaikis, A. Sureka, T. Hayashi, T. Taru, and T. Sasaki, "Space-division multiplexed transmission over 4200 km 3-core microstructured fiber," in *Proc. OFC/NFOEC* (2012), paper PDP5C.2.
4. S. Chandrasekhar, A. Gnauck, X. Liu, P. Winzer, Y. Pan, E. C. Burrows, B. Zhu, T. Taunay, M. Fishteyn, M. Yan, J. M. Fini, E. Monberg, and F. Dimarcello, "WDM/SDM transmission of 10 x 128-Gb/s PDM-QPSK over 2688-km 7-core fiber with a per-fiber net aggregate spectral-efficiency distance product of 40,320 km.b/s/Hz," in *Proc. ECOC* (2011), paper Th.13.C.4.
5. H. Takahashi, T. Tsuritani, E. L. T. de Gabory, T. Ito, W. R. Peng, K. Igarashi, K. Takeshima, Y. Kawaguchi, I. Morita, Y. Tsuchida, Y. Mimura, K. Maeda, T. Saito, K. Watanabe, K. Imamura, R. Sugizaki, and M. Suzuki, "First demonstration of MC-EDFA-repeatered SDM transmission of 40 x 128-Gbit/s PDM-QPSK signals per core over 6,160-km 7-core MCF," Opt. Express **21**(1), 789–795 (2013).
6. A. Al Amin, A. Li, X. Chen, and W. Shieh, "LP01/LP11 dual-mode and dual-polarization CO-OFDM transmission on two-mode fibre," Electron. Lett. **47**(10), 606–608 (2011).
7. R. Ryf, S. Randel, A. H. Gnauck, C. Bolle, A. Sierra, S. Mumtaz, M. Esmaeelpour, E. C. Burrows, R. Essiambre, P. J. Winzer, D. W. Peckham, A. H. McCurdy, and R. Lingle, "Mode-division multiplexing over 96 km of few-mode fiber using coherent 6 x 6 MIMO Processing," J. Lightwave Technol. **30**(4), 521–531 (2012).
8. E. Ip, G. Milione, M. J. Li, N. Cvijetic, K. Kanonakis, J. Stone, G. Peng, X. Prieto, C. Montero, V. Moreno, and J. Liñares, "SDM transmission of real-time 10GbE traffic using commercial SFP + transceivers over 0.5km elliptical-core few-mode fiber," Opt. Express **23**(13), 17120–17126 (2015).
9. S. Iano, T. Sato, S. Sentsui, T. Kuroha, and Y. Nishimura, "Multicore optical fiber," in *Optical Fiber Communication, 1979 OSA Technical Digest Series* (Optical Society of America, 1979), paper WB1.
10. S. Berdagué and P. Facq, "Mode division multiplexing in optical fibers," Appl. Opt. **21**(11), 1950–1955 (1982).
11. J. N. Blake, S. Y. Huang, B. Y. Kim, and H. J. Shaw, "Strain effects on highly elliptical core two-mode fibers," Opt. Lett. **12**(9), 732–734 (1987).
12. B. Y. Kim, "Few-mode fiber devices," in *Proc. Optical Fiber Sensors Conference 88* (1988), pp. 146–149.
13. W. V. Sorin, B. Y. Kim, and H. J. Shaw, "Highly selective evanescent modal filter for two-mode optical fibers," Opt. Lett. **11**(9), 581–583 (1986).

#255290 Received 11 Dec 2015; revised 5 Feb 2016; accepted 6 Feb 2016; published 11 Feb 2016
(C) 2016 OSA

14. K. Y. Song, I. K. Hwang, S. H. Yun, and B. Y. Kim, "High performance fused-type mode-selective coupler using elliptical core two-mode fiber at 1550 nm," IEEE Photonics Technol. Lett. **14**(4), 501–503 (2002).
15. K. Y. Song, B. Y. Kim, "Broad-band LP02 mode excitation using a fused-type mode-selective coupler," IEEE Photonics Technol. Lett. **15**(12), 1734–1736 (2003).
16. R. Ismaeel, T. Lee, B. Oduro, Y. Jung, and G. Brambilla, "All-fiber fused directional coupler for highly efficient spatial mode conversion," Opt. Express **22**(10), 11610–11619 (2014).
17. G. Pelegrina-Bonilla, K. Hausmann, H. Sayinc, U. Morgner, J. Neumann, and D. Kracht, "Analysis of the modal evolution in fused-type mode-selective fiber couplers," Opt. Express **23**(18), 22977–22990 (2015).
18. J. N. Blake, B. Y. Kim, and H. J. Shaw, "Fiber-optic modal coupler using periodic microbending," Opt. Lett. **11**(3), 177–179 (1986).
19. B. Y. Kim, J. N. Blake, H. E. Engan, and H. J. Shaw, "All-fiber acousto-optic frequency shifter," Opt. Lett. **11**(6), 389–391 (1986).
20. A. Amphawan, "Holographic mode-selective launch for bandwidth enhancement in multimode fiber," Opt. Express **19**(10), 9056–9065 (2011).
21. G. Stepniak, L. Maksymiuk, and J. Siuzdak, "Binary-phase spatial light filters for mode-selective excitation of multimode fibers," J. Lightwave Technol. **29**(13), 1980–1987 (2011).
22. J.-F. Morizur, P. Jian, B. Denolle, O. Pinel, N. Barré, and G. Labroille, "Efficient and mode-selective spatial multiplexer based on multi-plane light conversion," in *Proc. OFC* (2015), paper W1A.4.
23. S. G. Leon-Saval, A. Argyros, and J. Bland-Hawthorn, "Photonic lanterns: a study of light propagation in multimode to single-mode converters," Opt. Express **18**(8), 8430–8439 (2010).
24. N. K. Fontaine, C. R. Doerr, M. A. Mestre, R. R. Ryf, P. J. Winzer, L. L. Buhl, Y. Sun, X. Jiang, and R. Lingle, Jr., "Space-division multiplexing and all-optical MIMO demultiplexing using a photonic integrated circuit," in *Proc. OFC/NFOEC* (2012), paper PDP5B.1.
25. K. J. Park, K. Y. Song, Y. K. Kim, and B. Y. Kim, "All-fiber mode division multiplexer optimized for C-band," in *Proc. OFC* (2014), paper M3K.2.
26. W. V. Sorin, B. Y. Kim, and H. J. Shaw, "Phase-velocity measurements using prism output coupling for single- and few-mode optical fibers," Opt. Lett. **11**(2), 106–108 (1986).
27. J. D. Love, W. M. Henry, W. J. Stewart, R. J. Black, S. Lacroix, and F. Gonthier, "Tapered single-mode fibres and devices. Part 1: Adiabaticity criteria," IEEE Proceedings J. **138**, 343–354 (1991).
28. A. Yariv, "Coupled-mode theory for guided-wave optics," IEEE J. Quantum Electron. **9**(9), 919–933 (1973).
29. M. J. F. Digonnet and H. J. Shaw, "Analysis of a tunable single mode optical fiber coupler," IEEE Trans. Microw. Theory Tech. **30**(4), 592–600 (1982).

1. Introduction

It has been widely discussed that the available transmission capacity from a single strand of optical fiber has reached its limit after the maximum use of time division multiplexing (TDM) and wavelength division multiplexing (WDM) approaches [1]. The only remaining physical dimension not fully utilized is considered to be the space dimension in a strand of optical fiber [2]. The two popular approaches to the space division multiplexing (SDM) that are intensively investigated are multi-core fiber (MCF) [3–5] and mode division multiplexing (MDM) [6–8]. The MCF approach uses optical fibers with multiple single-mode cores and the MDM approach uses few mode optical fiber (FMF) with a core that guides several spatial/polarization modes [9,10]. These techniques can potentially increase the channel capacity by almost an order of magnitude and seem to be promising solutions for overcoming the limitation imposed by the nonlinear effect in WDM systems [2]. In fact, the use of multiple guided modes as independent information channels had been proposed decades ago for their applications to communications and sensing [10–12]. In order to fully utilize the higher order modes (HOM) in FMF, devices are required to control the modes guided in the fiber including excitation, separation and controlled coupling of individual guided modes in a single strand of FMF [12,13]. In addition to some of the early works such as mode selective coupler [13–17] and long period grating [18,19], various techniques have been reported on the basis of holographic filter, phase plate, photonic lantern and integrated circuit [20–24]. We recently reported an all-fiber MDM based on cascaded mode selective couplers (MSC's) for a fiber that supports four spatial modes (LP_{01}, LP_{11}, LP_{21}, and LP_{02}) [25]. The device showed more than 70% of coupling efficiency and 10dB extinction ratio at wavelength λ = 1550 nm, but had a limited operating wavelength range. This was due to the mismatch in the dispersion of the single-mode fiber (SMF) and FMF. The important advantages of the all-fiber MDM is the low insertion loss (theoretically approaching zero) if properly matching SMF-FMF pair is

#255290 Received 11 Dec 2015; revised 5 Feb 2016; accepted 6 Feb 2016; published 11 Feb 2016
(C) 2016 OSA

used, and also the fact that the MDM can be constructed on the same fiber used for transmission. In this paper we report significant improvement in the operating wavelength range of an all-fiber MDM using SMF-FMF pairs having matched effective refractive indices (n_{eff}) over a wide wavelength range. This is an essential feature required for practical WDM systems.

2. Higher order mode coupling using mode selective couplers

In [13], W. V. Sorin et al. described the basic operating principle of a MSC. The coupler is side-polished type constructed by mating SMF and FMF. When the propagation constant, and therefore the n_{eff}, of the guided mode in the SMF matches that of a mode in FMF, an efficient coupling takes place between the two modes by evanescent field coupling. Ideally no coupling occurs to other modes in the FMF due to phase mismatch. Almost lossless coupling with high modal isolation was demonstrated using this method for a wavelength used for the experiments [13,25]. The key parameter in this device is the phase matching between the coupling modes that is not trivial to achieve especially when multiple modes need to be coupled separately using a given FMF. In our earlier work the n_{eff} of each HOM were tuned by properly tapering the FMF for each MSC in the cascaded MDM structure [25]. As depicted in the inset of Fig. 1, the FMF and the SMF were attached to quartz blocks and polished until only a few microns of cladding remains before mating the two blocks with index matching liquid in between. Light launched into the SMF input port couples to the FMF in the particular LP_{nm} mode that has the matching n_{eff}. Conversely if light is injected in the LP_{nm} mode in the FMF, all the light should appear in the SMF assuming the phase matching condition is satisfied. In order to get a broadband operation, the n_{eff}'s should be the same over a wide spectral range. When we used the standard SMF, its n_{eff} did not match with that of the FMF over the entire operating wavelength range and could not provide a broadband operation. Significant improvement is presented in this work as will be described in the next section. A different approach is based on fused tapered structure [14–17] that provides much better environmental stability but is difficult to make, especially in a cascade structure.

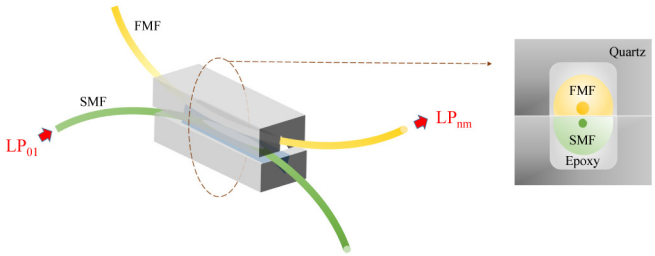

Fig. 1. Structure of a mode selective coupler (MSC) formed with a few mode fiber (FMF) and a single mode fiber (SMF). Inset shows cross section of MSC.

3. Fabrication of broadband mode selective couplers

The measurement of n_{eff} for fiber modes is essential for the fabrication of MSC's. The measurement was carried out using prism coupling method as shown in Fig. 2(a) [26]. Evanescent fields of the guided modes at the polished fiber region leak into the prism at different angles as a function of the n_{eff}'s. By measuring the angle θ, one can determine the n_{eff} of the mode as [26]

$$n_{eff} = \sqrt{n_p^2 - \sin^2\theta}, \tag{1}$$

where n_p is the refractive index of the prism. Figure 2(b) shows the measured intensity plot of the radiated light as a function of the height on the screen for the FMF modes at 1550 nm. From this data, we can calculate the accurate n_{eff} value for each mode. The FMF used for the

#255290 Received 11 Dec 2015; revised 5 Feb 2016; accepted 6 Feb 2016; published 11 Feb 2016
(C) 2016 OSA

experiment has a normalized frequency V = 4.54 at 1550 nm and 10.2 μm core diameter. With a highly Ge-doped (1.2%) step index core, the n_{eff} for the guided modes are well separated with the exception of $LP_{21}$and LP_{02}. The FMF guides four linearly polarized (LP) modes (LP_{01}, LP_{11}, LP_{21} and LP_{02} modes) and their n_{eff} measured by the prism coupling method is plotted in Fig. 3(a) for the wavelength range between 1515 nm and 1590 nm. As can be seen in the Fig. 3(a) the wavelength dependence of the n_{eff} is almost linear but with different slopes for the different modes. As a reference, the difference in n_{eff} at the two wavelengths of 1515 nm and 1590 nm for LP_{01}, LP_{11}, LP_{21} and LP_{02} mode are 1.1×10^{-3}, 1.5×10^{-3}, 1.7×10^{-3} and 1.8×10^{-3}, respectively.

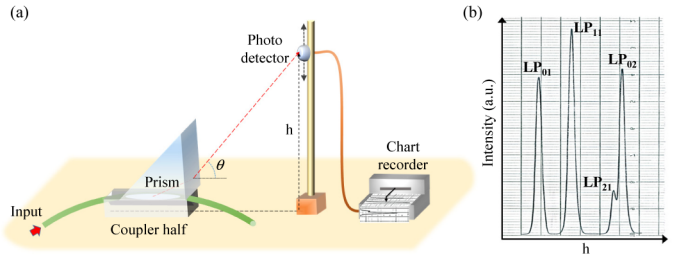

Fig. 2. (a) Experimental setup for prism coupling method. (b) Recorded output from a few mode fiber coupler half. Different modes in the few mode fiber radiates in different angle.

In an ideal case, three different SMFs that have matching n_{eff}'s with those of the HOM of the FMF over a wide wavelength range should be used. In practice we used SMFs with high numerical aperture (NA) that have approximately matching wavelength dependence of n_{eff} ($dn_{eff}/d\lambda$) with that of the FMF and fine-tuned the n_{eff} values by tapering to match with that of the HOMs in the FMF. As an example, Fig. 3(b) shows the wavelength dependence of n_{eff} for LP_{02} mode of the FMF (red square) compared with that of the resultant SMF mode (navy triangle) showing a good match. For comparison, the values for a standard communication SMF is shown where a big mismatch can be seen (green dot). This feature results in a big difference in the operation bandwidth of the MSC as described in the next section. The SMFs tested for the experiment had nominal NAs in the range of 0.2-0.3. The tapering was done by flame heating and pulling that reduces n_{eff} [27]. Proper taper diameter was calculated by numerical simulations of the mode in the SMF. The SMF was tapered approximately to the target diameter where n_{eff} of 1550 nm became identical with that of the desired HOM mode in the FMF. Optimum taper diameter was determined after experimental fine tuning.

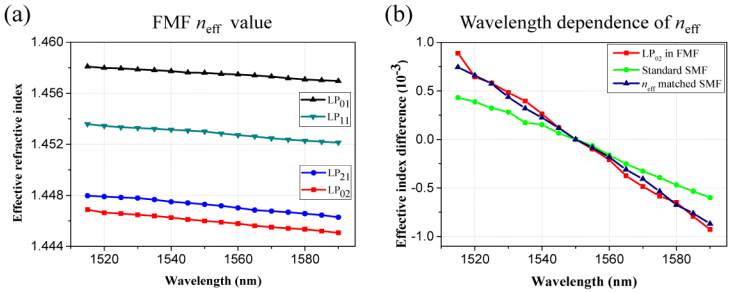

Fig. 3. (a) n_{eff} of radiated modes in FMF. Each radiated mode is measured by prism coupling method with 5 nm spacing from 1515 nm to 1590 nm. (b) Wavelength dependence of n_{eff} of LP_{02} (red square), standard SMF (green dot) and SMF with matched n_{eff} (navy triangle) from 1515 nm to 1595 nm.

#255290 Received 11 Dec 2015; revised 5 Feb 2016; accepted 6 Feb 2016; published 11 Feb 2016
(C) 2016 OSA

4. Mode coupling efficiency

Mode coupling between HOM in FMF and LP_{01} mode in SMF is described by the coupled mode theory [28]:

$$P_{out} = P_{in} \frac{\kappa^2}{\kappa^2 + \delta^2} \sin^2 \left[\sqrt{\left(\kappa^2 + \delta^2\right)} z \right]. \quad (2)$$

Here P_{in} and P_{out} are input and coupled power, respectively, κ is a coupling constant, z is interaction length and $\delta = \Delta\beta / 2$ is the propagation constant (β) mismatch between the modes of FMF and SMF. According to Eq. (2), difference in n_{eff} between target mode of the FMF and LP_{01} mode in the SMF should be minimized for maximum power coupling. For instance, when z is set as 1.6 mm (which corresponds to our case) [29] and $\kappa z = \pi/2$ at 1550 nm, δ should be less than 2.2×10^{-4} to achieve more than 80% coupling. In this work, coupling efficiency (C_e) to target mode is defined by the ratio between output power in the target mode in FMF and input power of LP_{01} mode in SMF. As an example, Fig. 4 shows the experimental results of C_e into the LP_{02} mode of the FMF from the LP_{01} mode from Fig. 4(a) standard SMF and Fig. 4(b) n_{eff} matched SMF. As expected, the bandwidth for mode selective coupling increased significantly by using n_{eff} matched SMF. The maximum C_e for the two cases exceeded 80%. The C_e to the LP_{02} mode in the device with n_{eff} matched SMF at 1535 nm was 83%. The rest of input power went to unwanted LP_{21} mode (8.2%), splicing loss (nominally 6-10%), and some did not couple and remained in the SMF (typically 1%). The measurements were made in the following process. The input power was measured at the laser source pigtail for the LP_{02} MSC using a power meter. The total output power from the FMF was measured by using a power meter that may also contain signals in unwanted modes. Then a fiber loop was formed in the output FMF to induce bending loss. A separate measurement showed a loss of 20dB for the LP_{02} mode for the loop diameter of 20 mm without significantly affecting other modes in the FMF. The LP_{21} mode showed less than 0.1dB bending loss at the loop diameter of 20 mm and required 6 mm loop diameter to induce 17dB loss. The bending loss for the LP_{01} and the LP_{11} modes were negligible. The degradation of C_e in L band in Fig. 4(b) is considered to be from the finite spectral bandwidth of evanescent field coupler as well as imperfect n_{eff} matching [29].

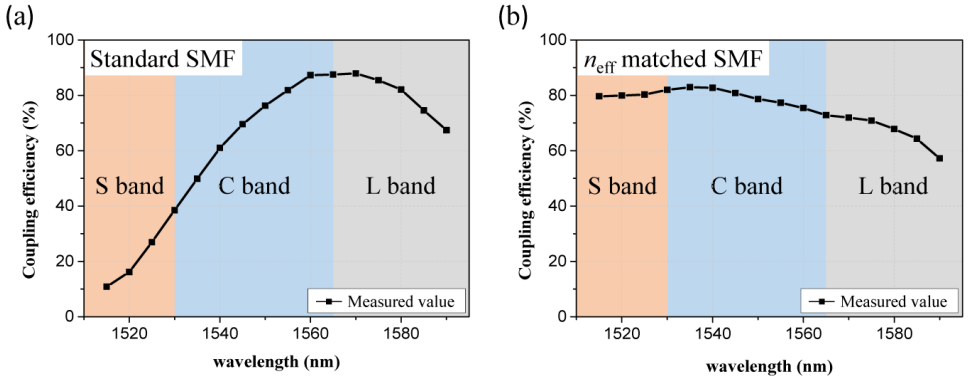

Fig. 4. Measured coupling efficiency for (a) LP_{02} mode coupled from standard SMF, (b) LP_{02} mode coupled from n_{eff} matched SMF.

5. Mode-division multiplexer

We constructed a four-mode MDM by cascading three MSC's as shown in Fig. 5. In order to prevent the splicing loss and unwanted mode coupling at the splices, we used an unbroken strand of FMF for all the three MSC's. The input ports for the four modes are pigtailed with

#255290 Received 11 Dec 2015; revised 5 Feb 2016; accepted 6 Feb 2016; published 11 Feb 2016
(C) 2016 OSA

standard communication SMF to make them compatible with communications systems. In order to remove undesired optical signal in the LP_{02} mode coupled at the LP_{21} MSC, we inserted a mode stripper between the LP_{21} and the LP_{02} MSC that was formed by a fiber loop with 20 mm diameter. There was no need to include a mode stripper between the LP_{11} and the LP_{21} MSC's because we could not measure any coupling to the LP_{21} or the LP_{02} modes that is believed to be from a large separation of n_{eff} between the LP_{11} mode and higher order modes ($>5.5 \times 10^{-3}$) as shown in Fig. 3(a).

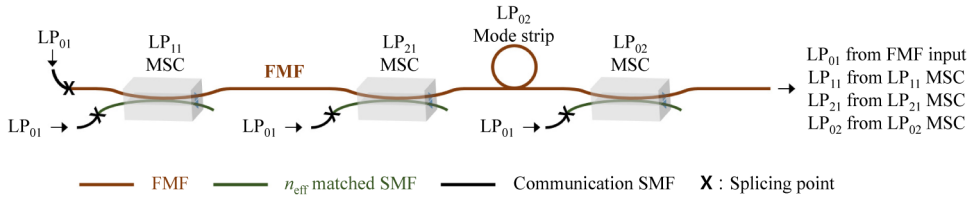

Fig. 5. Cascaded mode selective couplers to form a mode division multiplexer.

The extinction ratio R_E of MSC is also an important parameter and is defined by

$$R_E = 10\log\left(P_{target}/P_{other}\right). \tag{3}$$

Here P_{target} is the optical power coupled to the desired mode and the P_{other} is the optical power coupled to unwanted modes. The measurement of the R_E's for the LP_{01} and the LP_{11} modes should be made during the fabrication process of the MSC's, since it becomes very complicated to measure them after the MDM is assembled. In order to determine the R_E, light is launched to one input port and the optical power is measured at the output port before and after unwanted modes are stripped as described in the previous section. The mode stripping was performed by fiber bending or using index matching liquid on the coupler halves following each MSC being measured. For this purpose, the MSC's were assembled in the order of LP_{11}, LP_{21} and LP_{02} modes. We confirmed that the assembly process of the LP_{21} and the LP_{02} MSC's did not induce additional loss for the LP_{01} and the LP_{11} modes. Figures 6(a)-6(d) show the C_e and R_E for each coupled mode of the constructed MDM, where high performance operation over S, C and L bands can be confirmed. The far-field radiation patterns for each coupled mode were recorded by using a 1550 nm light source and an IR beam profiler which are shown in the inset of Fig. 6. It can be seen in Fig. 6(a)-6(d) that the performance in the C_e and R_E for the LP_{21} and the LP_{02} modes are poorer compared to the LP_{01} and the LP_{11} mode cases. The reason for this is due to the small separation of the n_{eff} between the LP_{21} and the LP_{02} modes as shown in Fig. 3(a) that makes it difficult to separate based on phase matching within such a short coupling length (~1 mm) in the MSC. Therefore non-negligible amount of signal couples to the unwanted modes that degrades the C_e and the R_E simultaneously. Ideally the extinction ratio for the LP_{21} mode should be 20dB after the mode stripper that did not agree with the experimental result. It is thought to be from an imperfect mode stripping at the fiber loop in the packaged device, and further investigation is under way. Table 1 summarizes C_e to the desired and unwanted modes for the MDM tested at 1550 nm. Another point that should be mentioned is that the C_e in the evanescent directional coupler structure has a finite wavelength bandwidth that would result in a variation of C_e over wavelength. In order to improve further the performance of the all-fiber MDM, optimized fiber design for both the FMF and SMF is needed with clear separation of n_{eff} for FMF with well-matched n_{eff} for SMF.

#255290 Received 11 Dec 2015; revised 5 Feb 2016; accepted 6 Feb 2016; published 11 Feb 2016
(C) 2016 OSA

Table 1. Coupling efficiencies of desired mode and unwanted mode at 1550 nm

Mode	Coupling efficiency (%)			
	LP_{01}	LP_{11}	LP_{21}	LP_{02}
Desired mode	90.4	78.9	66.2	78.7
Unwanted mode	1.7 (mainly LP_{11})	0.1 (mainly LP_{01})	10.2 (mainly LP_{02})	9.9 (mainly LP_{21})

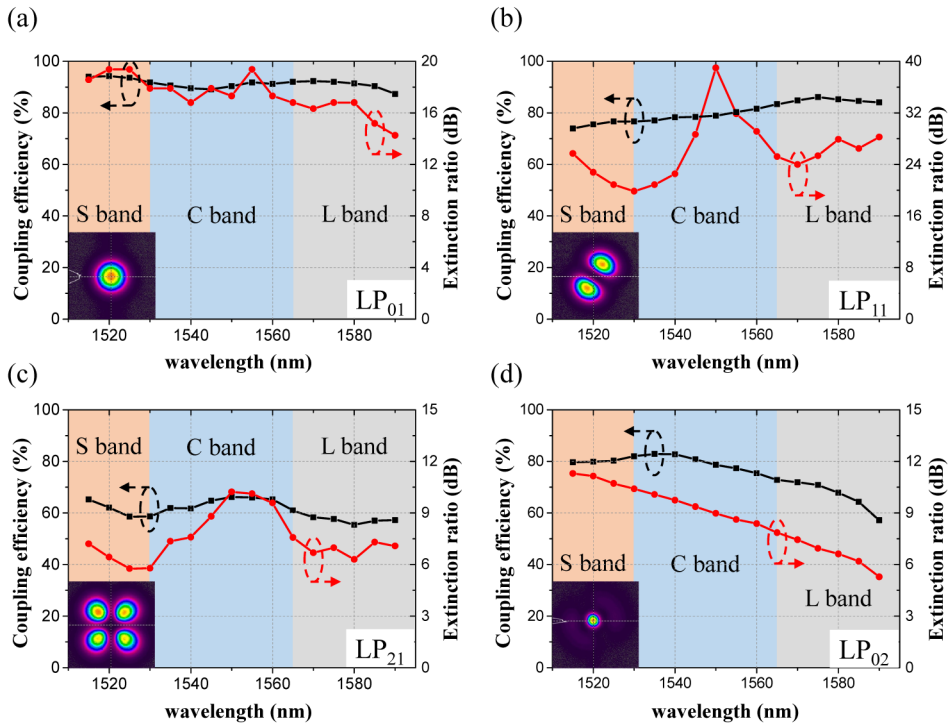

Fig. 6. (a)-(d) Coupling efficiency (black square) and extinction ratio (red dot) for the LP_{01}, LP_{11}, LP_{21} and LP_{02} spatial modes, respectively. Insets show corresponding far-field intensity patterns.

6. Conclusion

We demonstrated an all-fiber mode division multiplexer based on cascaded mode selective couplers with broad bandwidth. The coupling efficiency over the entire wavelength range between 1515 nm and 1590 nm ranged from > 87% for the LP_{01} mode and, in the worst case, >55% for the LP_{21} mode. The significantly improved performance was achieved by matching the n_{eff} over the operation wavelength of few mode fiber and single mode fiber. This device could be useful for further development of high bandwidth mode division multiplexed communication systems.

Acknowledgments

This research was supported by Basic Science Research Program through the National Research Foundation of Korea (NRF) funded by the Ministry of Science, ICT & Future Planning (2013R1A1A2064061).

#255290 Received 11 Dec 2015; revised 5 Feb 2016; accepted 6 Feb 2016; published 11 Feb 2016

(C) 2016 OSA

152.78.74.132 (6) 2018-05-15 12:30:29